

# MRPoS: Mixed Reality-Based Robot Navigation Interface Using Spatial Pointing and Speech with Large Language Model

Eduardo Iglesias<sup>†1</sup>, Masato Kobayashi<sup>†1,2\*</sup>, Yuki Uranishi<sup>1</sup>

**Abstract**—Recent advancements have made robot navigation more intuitive by transitioning from traditional 2D displays to spatially aware Mixed Reality (MR) systems. However, current MR interfaces often rely on manual “air tap” gestures for goal placement, which can be repetitive and physically demanding, especially for beginners. This paper proposes the Mixed Reality-Based Robot Navigation Interface using Spatial Pointing and Speech (MRPoS). This novel framework replaces complex hand gestures with a natural, multimodal interface combining spatial pointing with Large Language Model (LLM)-based speech interaction. By leveraging both information, the system translates verbal intent into navigation goals visualized by MR technology. Comprehensive experiments comparing MRPoS against conventional gesture-based systems demonstrate that our approach significantly reduces task completion time and workload, providing a more accessible and efficient interface. For additional material, please check: <https://mertcooking.github.io/mrpos>

## I. INTRODUCTION

Autonomous mobile robots (AMRs) have emerged as a transformative technology within domestic, healthcare, and industrial fields. Notably, with the advent of the Robot Operating System (ROS) [1], robotic navigation has been highly abstracted, requiring users only to input a target pose, and the system will autonomously navigate to the target.

Current tools for generating and visualizing goal poses typically rely on these modalities: 2D computer displays, natural language (speech or text), or MR gestures. However, each approach possesses inherent limitations. Conventional 2D interfaces reduce operational efficiency by forcing users to constantly shift their attention between a screen and the real environment. Language-centric interfaces, despite leveraging LLM for high-level reasoning, struggle with spatial grounding [2], as describing precise coordinate and orientation often introduces ambiguity. Recent works attempt to bridge this perception-action gap using Vision-Language-Action (VLA) models [3]. Conversely, while MR offers spatial precision necessary to define target poses accurately, relying exclusively on mid-air hand gestures to specify target poses for too long induces a high overall workload [4].

To address these limitations, this paper introduces MRPoS, a novel framework that optimizes goal pose generation by fusing speech with MR. We propose that these modalities are complementary: MR mitigates the spatial blindness of LLMs, while the semantic power of natural language reduces the workload inherent in MR manipulation. This hybrid approach allows user to simultaneously define a target location via spatial pointing while specifying the desired orientation through

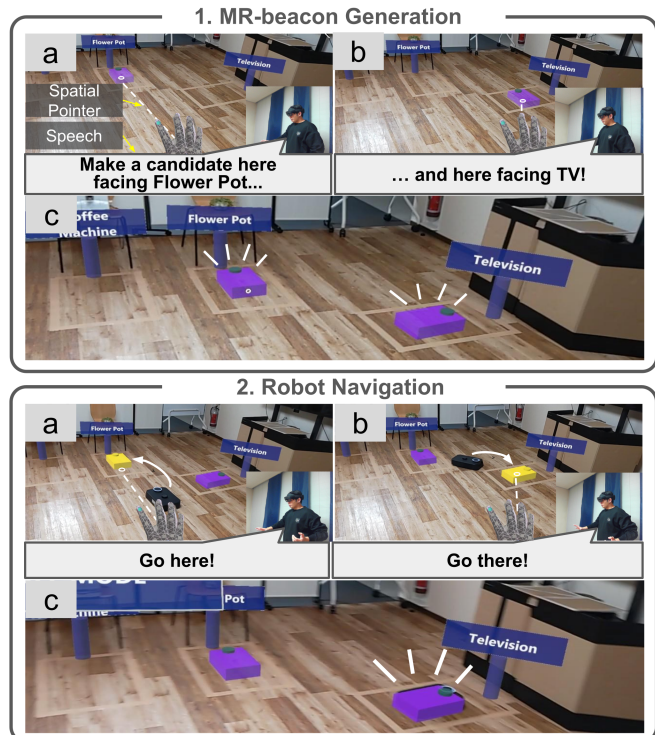


Fig. 1: **MRPoS Workflow**. The workflow is divided into 2 phases, which are MR-beacon Generation and Robot Navigation. (1-a, 1-b) shows the MR-beacon generation by using spatial pointer and voice. (1-c) shows the final state after the generation. (2-a, 2-b) shows the robot navigation towards the created MR-beacon. (2-c) shows the final state.

intuitive voice commands (Fig. 1). MRPoS features four core functionalities: Add to place single or multiple MR-beacons, Edit to adjust the MR-beacon’s location and rotation, Go to dispatch the robot to the MR-beacon, and Delete to remove an MR-beacon from the environment.

Our contributions are summarized as follows:

- This paper introduces MRPoS, a multimodal system that streamlines multiple robotic goal poses generation by combining natural language for intuitive interaction with MR spatial pointing for precise spatial grounding.
- This paper proposes an architecture that independently interprets voice and pointer inputs before integrating them to calculate the final target pose for multiple goals.
- We conducted experiments to compare MRPoS with the baseline gesture-based MR interface, showing the advantages in workload and operational efficiency.

<sup>†</sup> Equal Contribution, <sup>1</sup> The University of Osaka, <sup>2</sup> Kobe University, <sup>\*</sup> corresponding author: [kobayashi.masato.cmc@osaka-u.ac.jp](mailto:kobayashi.masato.cmc@osaka-u.ac.jp)

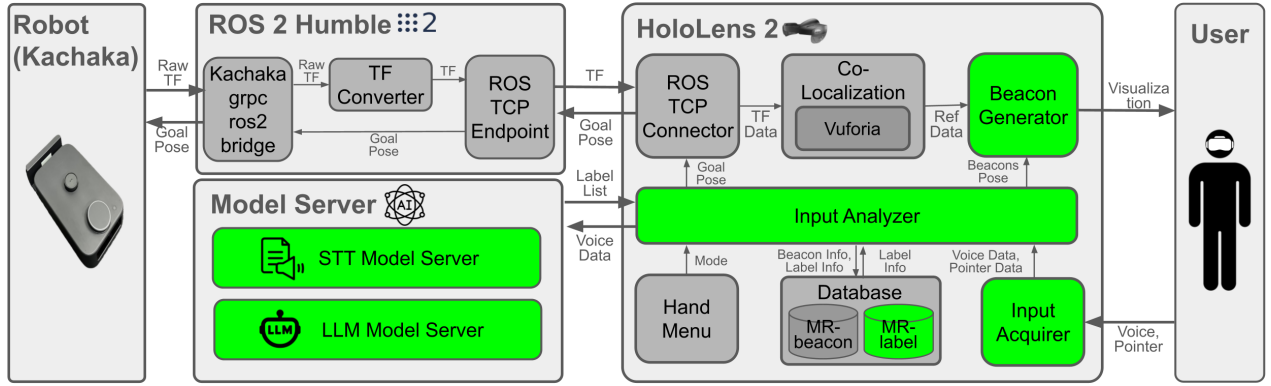


Fig. 2: **System Design Diagram.** Our system consists of four main modules: the HoloLens 2, serving as the user interface to acquire, analyze, and visualize MR-beacons; ROS 2, acting as a bridge between the HoloLens 2 and the robot; a Model Server to process user voice data; and the robot itself. Components highlighted in green represent our novel contributions.

## II. RELATED WORK

### A. MR Robot Navigation Interface

Integrating MR into robot navigation significantly increases operational efficiency by aligning the robot’s internal map with the user’s physical environment. Applications vary widely, from visualizing motion intent, safety distance [5], [6] to defining restricted zones [7] and manual operation [8].

For autonomous navigation, MRNaB [9], which is the improvement of ARviz [10], enhances traditional 2D SLAM-based occupancy grids by projecting them into the HoloLens 2 environment. This system enables visualization of the goal pose by using a persistent MR-beacon similar to the real object, which projects the navigation goals via “air tap” hand gestures. Other studies have also explored the use of discrete waypoints as a primary modality for setting navigation objectives [11]–[14]. Alternative interfaces include the use of a drag-and-drop interface [15]–[17] and also eye movement [18].

Despite the advancements, these developments also face several challenges :

- **Serialized Waypoint Generation:** Traditionally, defining a goal pose’s position and orientation is a sequential process. This introduces operational latency when generating multiple navigation candidates simultaneously.
- **Elevated Workload:** Relying on specialized mid-air hand gestures imposes a steep learning curve which increases ergonomic strain and cognitive demand.

This research addresses these limitations by integrating a speech interface with LLMs to reduce workload through natural language interaction. Furthermore, we parallelize these generation process by utilizing natural language for orientation (rotation) and MR spatial pointers for position.

### B. Language-Centric Robot Navigation

LLMs have enabled more natural language interaction for navigation-related tasks, ranging from dialogue-based reasoning and planning [19]–[23] to language-driven navigation benchmarks and policies [24]–[27]. However, language-only interfaces often face two practical issues in navigation: (1)

TABLE I: Qualitative design-space summary of robotic navigation interface paradigms.

	Gesture-Based MR	Language-Centric	MRPoS (Hybrid)
Natural Language Interaction	✗	✓	✓
Visual Intent Transparency	✓	✗	✓
Precise Spatial Grounding	✓	✗	✓
Low Workload	✗	✓	✓

Gesture-based MR refers to [7], [9]–[12], [15]. Language-centric refers to [19]–[21], [24], [25], [29].

limited spatial grounding, where precise goal coordinates and orientations are difficult to specify unambiguously, and (2) reduced intent transparency, due to the user’s inability to verify the target goal pose in the physical environment prior to execution. Multimodal approaches (e.g., combining language with sketches or visual inputs) partially address these issues [3], [28], but their interaction and visualization differ from MR-based goal specification.

In this paper, we treat language primarily as an *auxiliary modality* to reduce interaction burden in the MR interface. MRPoS combines MR pointing (for spatial grounding) with LLM-processed speech (for expressing orientation) while keeping the goal pose visible and verifiable in situ. Thus, our evaluation focuses strictly on an MR-to-MR comparison.

## III. SYSTEM DESIGN

The system design, illustrated in Fig. 2, integrates the Kachaka robot and the HoloLens 2 through a ROS 2 middleware framework. Within this ecosystem, ROS 2 is employed to subscribe to the robot’s transform (TF) data and command goal poses. The HoloLens 2 serves as the primary interface for capturing and processing user information, which is then utilized to determine and transmit the target pose. To facilitate natural language interaction, an independent server is implemented to host the Speech-To-Text (STT) and the Large Language Model (LLM) services. Bidirectional communication between the ROS 2 and the HoloLens 2 is established via the ROS-TCP-Connector, while the HoloLens 2 interacts with the STT and LLM servers through standard HTTP requests by sending POST requests.

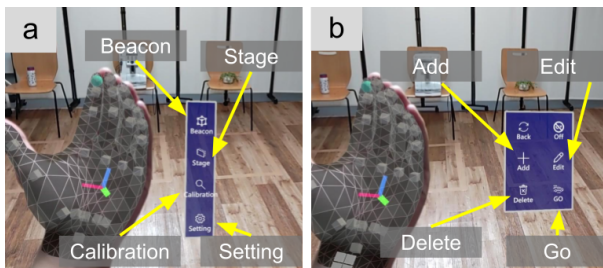


Fig. 3: **Hand Menu.** (a) The primary layout of the hand menu. (b) The Beacon submenu, accessed via the main menu.

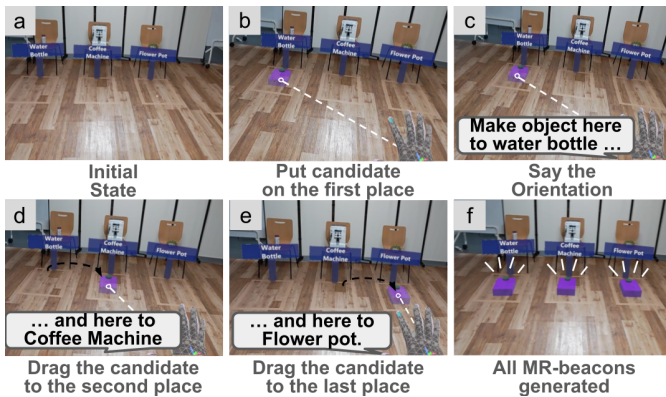


Fig. 4: **Add Function (Multiple Objects).** (a) Initial empty environment. (b) User positioning the first MR-beacon candidate. (c) User specifying orientation toward the water bottle via speech by specifying the name. (d, e) User repeating the same process for the coffee machine and flower pot simultaneously. (f) Final state with three generated MR-beacons.

To access the MR-beacon functionalities for robot navigation, a hand menu is invoked using the “Hand Constraint Palm Up” gesture, as illustrated in Fig. 3. This menu provides access to three primary menu: the Beacon, Stage, and Calibration buttons. The Stage button is used for experimental control, while the Calibration button allows for the adjustment of the user’s minimum audio volume threshold. Upon selecting the Beacon button, the interface expands into six specialized functions: Back, Off, Add, Edit, Go, and Delete. The Back button returns the user to the main menu, and the Off button deactivates all MR-beacon functionalities. The core operations of the system, Add, Edit, Go, and Delete functions are executed through their respective buttons.

#### A. Add Function

The *Add* function generates MR-beacons directly onto the floor plane. Upon pressing the corresponding button, the system enters the “Add Mode”, which supports the creation of either a single or a sequence of multiple target poses through a continuous pointing and speech workflow. As shown in Fig. 4, the user first points to a desired location on the floor, dynamically guiding a semi-transparent candidate MR-beacon in real-time. Upon finalizing the location, the user issues a voice command to specify the robot’s orientation, generating a persistent MR-beacon at that pose. For multiple destinations,

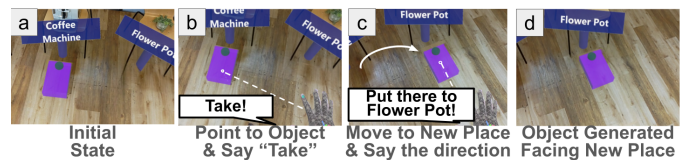


Fig. 5: **Edit Function.** (a) Initial state with an MR-beacon. (b) User selecting the MR-beacon via spatial pointing. (c) User relocating it and specifying a new orientation (flower pot) via speech. (d) Final state of the modified MR-beacon.

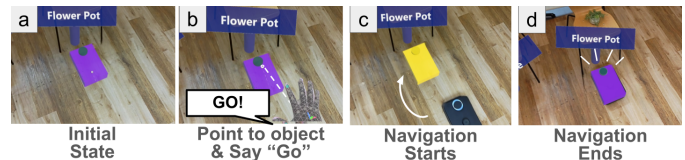


Fig. 6: **Go Function.** (a) Initial state with an MR-beacon. (b) User pointing to the target MR-beacon and issuing the “Go” command. (c) Robot navigating to the target. (d) Successful arrival at the destination.

the user simply maintains this interaction loop, seamlessly shifting the pointer to new locations and issuing corresponding commands for each subsequent target.

#### B. Edit Function

The Edit function is designed to modify the spatial coordinates and rotation of an existing MR-beacon. Upon activating this feature, the system transitions into “Edit Mode”, a two-step procedure comprising beacon selection and repositioning, as shown in Fig. 5. To select the target, the user directs the spatial pointer toward a previously instantiated MR-beacon. When the cursor intersects the object, the user says “Take”, effectively attaching the MR-beacon to the pointer’s trajectory. To finalize the relocation, mirroring the workflow of “Add Mode”, the user designates the new target coordinates via spatial pointing while simultaneously saying the robot direction to define the updated orientation.

#### C. Go Function

The “Go” function navigates the robot to the precise position and orientation of a designated MR-beacon. Pressing the “Go” button transitions the system into “Go Mode”, as illustrated in Fig. 6. First, the user directs the spatial pointer toward an instantiated MR-beacon. Once the cursor intersects the object, the user issues the “Go” voice command, prompting the robot to initiate movement toward the target.

#### D. Delete Function

The “Delete” function is used to remove an existing MR-Beacon from the environment. Pressing the “Delete” button transitions the system into “Delete Mode”, as illustrated in Fig. 7. First, the user aims the spatial pointer at a previously instantiated MR-Beacon. Once the cursor intersects the target object, the user issues the “Delete” voice command, which immediately removes the beacon from the physical space.

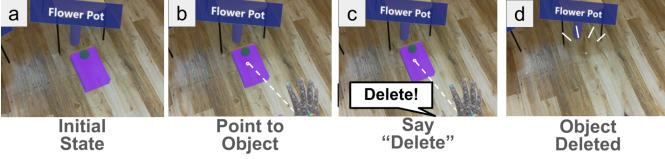


Fig. 7: **Delete Function.** (a) Initial state with an MR-beacon. (b) Pointing to select the target MR-beacon. (c) Issuing the “Delete” command to remove the MR-beacon. (d) Final state with the MR-beacon removed.

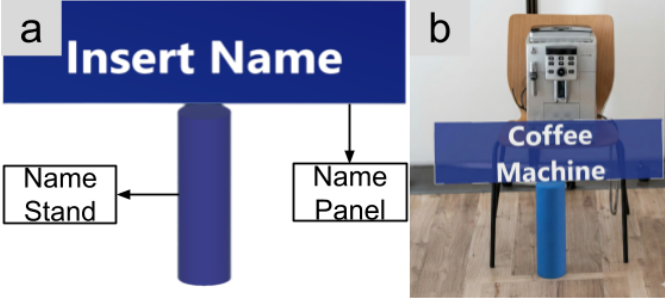


Fig. 8: **MR-label.** (a) illustrates the components of the MR-label, which consists of a name panel to display the location’s name and a name stand to mark its position on the floor. (b) demonstrates the deployment of MR-labels in a real-world

## IV. SYSTEM IMPLEMENTATION

### A. MR-label

The MR-label is utilized within the system to assign a unique semantic name to a specific coordinate in the physical environment. This designated location then functions as a persistent directional reference, which the system uses to determine the exact orientation the MR-beacon must adopt upon the generation. The specific structure of these MR-labels and their implementation within the application interface are illustrated in Fig. 8.

### B. Database

Separate databases are implemented for both the MR-labels and the MR-beacons to ensure persistent access to their spatial and semantic data. For the MR-labels, the database stores three primary attributes: (1) ID, a unique identifier generated via a Globally Unique Identifier (GUID), (2) Name, the semantic annotation displayed on the object’s name panel, and (3) Location, a 3D vector  $(x, y, z)$  representing the coordinates relative to the global image target.

Similarly, the MR-beacons are stored with the following attributes: (1) ID, a unique identifier generated using a GUID, (2) Location, a 3D vector  $(x, y, z)$  defining the MR-beacon’s position, and (3) Rotation, a vector or Quaternion  $(x, y, z, w)$  representing the MR-beacon’s orientation. All spatial data for both databases is calculated and stored relative to the global image target to maintain coordinate consistency.

### C. Input Acquirer

To provide a seamless user experience without requiring manual triggers, we implemented a Voice Activity Detector

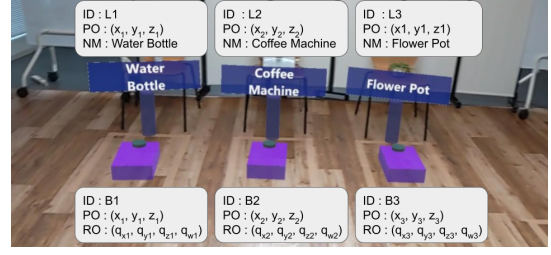


Fig. 9: **Database.** The MR-label database logs the ID, position (PO), and name (NM). The MR-beacons database logs the ID, position (PO), and rotation (RO).

### Algorithm 1 User Input Analysis

---

```

1: Input: Hand Menu, Input Acquirer, Label DB
2:  $currentMode \leftarrow$  Hand Menu
3: if  $currentMode$  is Inference Action then
4:    $(voiceData, pointerData) \leftarrow$  Input Acquirer
5:    $labelNameList \leftarrow$  AnalyzeVoice( $voiceData$ )
6:    $clusterList \leftarrow$  AnalyzePointer( $pointerData$ )
7:    $labelInfo \leftarrow$  Label DB
8:   CalculatePose( $labelNameList, clusterList, labelInfo$ )
9: else
10:   $pointerData \leftarrow$  Input Acquirer
11:   $beacon \leftarrow$  Identify MR Beacon( $pointerData$ )
12:  Execute Command( $beacon, currentMode$ )
13: end if

```

---

(VAD). This component monitors audio input to detect the onset of speech (voice detection) and the completion of a command (silence detection) using a predefined threshold.

Once the voice detection is triggered, the system simultaneously captures the audio stream and the user’s current spatial pointer coordinates on the floor. To ensure high precision for the pointer analysis process, the pointer data is sampled every 0.1 seconds. After the silence detection is triggered, the system then analyzes the collected voice and pointer data to be further processed based on the current mode.

### D. User Input Analyzer

The user input analysis algorithm is described in Alg. 1. Based on the current mode from the hand menu, the system categorizes the expected actions from the user into two types, which are the Non-Inference and Inference actions.

Non-Inference actions (e.g., Delete and Go functions) are deterministic and do not require an LLM model, which means they rely solely on the user’s pointer coordinate. These actions requires system to detect which MR-beacon did it collide and do the process according to the mode.

Inference actions (e.g., Add Mode) required both synchronized voice and pointer data. This data is processed independently through Voice Analyzer and Pointer Analyzer, before the system integrates these outputs with a predefined MR-label list from the database to calculate the corresponding pose.

1) *Voice Analyzer*: Voice Analyzer requires two primary components: an STT model and an LLM model. The STT model uses *faster-whisper* with *small.en* model in order to convert raw audio data into text, which is then processed by the LLM to identify the MR-labels for each MR-beacons as a JSON-formatted string. The string is subsequently parsed by a

---

**Algorithm 2** Clustering Algorithm
 

---

```

1: Input: pointList
2:  $M \leftarrow \text{GetSize}(\text{pointList})$ 
3: for  $i \leftarrow 1$  to  $M$  do
4:    $\text{curPoint} \leftarrow \text{pointList}[i]$ 
5:   if  $\text{Dist}(\text{curPoint}, \text{curCentroid}) \leq D_{th}$  then
6:     Recalculate Cluster Centroid
7:     Cluster Size Increases by 1
8:   else
9:     Record Current Cluster
10:    Create New Cluster Size 1
11:   end if
12: end for
13: Record Last cluster

```

---

**Algorithm 3** MR-beacon Pose Calculation
 

---

```

1: Input: labelNameList, clusterList, labelInfo
2:  $N \leftarrow \text{GetSize}(\text{labelNameList})$ 
3:  $\text{biggestCluster} \leftarrow \text{GetTopNBigestCluster}(\text{clusterList})$ 
4:  $\text{locationList} \leftarrow \text{SortByTime}(\text{biggestCluster})$ 
5:  $\text{AllPose} \leftarrow \text{empty list}$ 
6: for  $i \leftarrow 1$  to  $N$  do
7:    $\text{curLoc} \leftarrow \text{LocationList}[i]$ 
8:    $\text{curLabel} \leftarrow \text{labelNameList}[i]$ 
9:    $\text{curLabelLoc} \leftarrow \text{GetCurrentLabelInfo}(\text{curLabel}, \text{labelInfo})$ 
10:   $\text{curRot} \leftarrow \text{FindAtan}(\text{curLoc}, \text{curLabelLoc})$ 
11:   $\text{curPose} \leftarrow \text{ConstructPose}(\text{curLoc}, \text{curRot})$ 
12:  Add  $\text{curPose}$  to  $\text{AllPose}$ 
13: end for
14: return  $\text{AllPose}$ 

```

---

JSON converter to a list of the MR-label name, which is then used to calculate each of the MR-beacons' pose. The model we used for LLM model is *meta-llama/Llama-3.1-8B-Instruct*.

2) *Pointer Analyzer*: Pointer Analyzer analyzes the user's spatial pointer information to determine the location of all possible MR-beacons. The algorithm used to determine the cluster from the pointer data is shown in Alg. 2.

The algorithm processes data points one by one, identifying and classifying them by maintaining a running average of the current cluster as its centroid. For each new point, the algorithm checks whether the point is inside the current centroid by calculating its distance from the active centroid whether it is within a certain threshold  $D_{th}$ . If the point falls within, it is included in the cluster, updating the cluster centroid again while increasing the size of the cluster by 1. Meanwhile, if a point falls outside, the algorithm records the current cluster, saves its final centroid to a list and size, and immediately starts a new cluster using the outlier as the first point. The extracted cluster data is then used to calculate the pose of each of the MR-beacons. This procedure maintains a linear time complexity of  $O(n)$ .

3) *Pose Calculation*: Finally, the system determines the quantity, position, and rotation of the MR-beacons by integrating the voice analyzer's MR-label list with the pointer analyzer's clusters. As shown in Alg. 3, first, the number of beacons to be generated,  $N$ , is defined by the quantity of detected MR-labels from voice analyzer. To capture the relevant spatial data while preserving the user's intent sequence, the system extracts the  $N$  largest pointer clusters and sorts them chronologically. For each  $i$ -th MR-beacon (from 1 to  $N$ ), its position is directly assigned to the  $i$ -th sorted cluster's location. Its rotation (yaw) is oriented

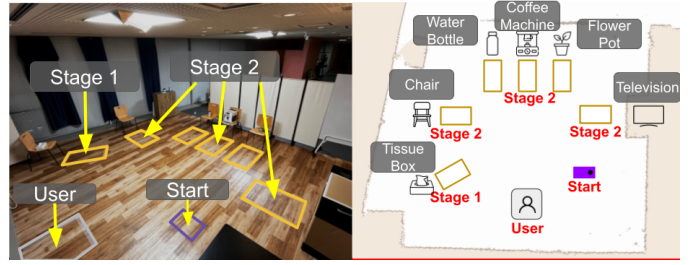


Fig. 10: **Experiment Environment.** (a) shows the figure of the real-world experiment environment. (b) shows the figure of the experiment environment from 2D map SLAM.

toward the corresponding MR-label by calculating the atan2 of the displacement vector between the MR-beacon's position and the MR-label's database coordinates. Finally, the system outputs these combined positions and rotations as target poses to be instantiated as the MR-beacon.

### E. Unity-ROS Integration

1) *Communication with ROS 2 and Model*: A ROS-TCP-Connector is employed to facilitate communication between the HoloLens 2 and ROS 2. This bridge enables the exchange of robotic data, including Transform (TF) data for spatial colocalization and goal pose data for autonomous navigation.

To maintain a modular architecture, the STT and LLM models are hosted on an independent server using the FastAPI framework via the HTTP protocol, by sending POST requests containing the audio file for the STT model and the transcribed text for the LLM to retrieve the MR-label names.

2) *Co-Localization*: To align the coordinate systems of ROS 2 and the HoloLens 2, a co-localization process is required. Utilizing Vuforia, a reference object (QR Code) is registered in the Vuforia database to act as the reference point for all MR-objects in HoloLens 2 and also corresponds to the ROS map origin. This results in a simplified coordinate transformation between both coordinate systems.

## V. EXPERIMENTS

To evaluate the effectiveness of the proposed system, we conducted an experiment comparing the proposed MRPoS system with MRNaB [9] as the gesture-based MR system baseline. The experiment was conducted twice, once for the MRNaB and MRPoS systems per participant, in a counterbalanced order. Sixteen participants were involved in the experiments. Most of whom had no prior experience with ROS or VR/AR/MR.

### A. Experiment Setup

Fig. 10 illustrates the experimental environment, which was designed to simulate a typical household setting. The environment includes common items such as a tissue box, chair, water bottle, coffee machine, flower pot, and television. The task was to navigate the robot to predetermined areas, marked by tape with the direction facing to the closest object.

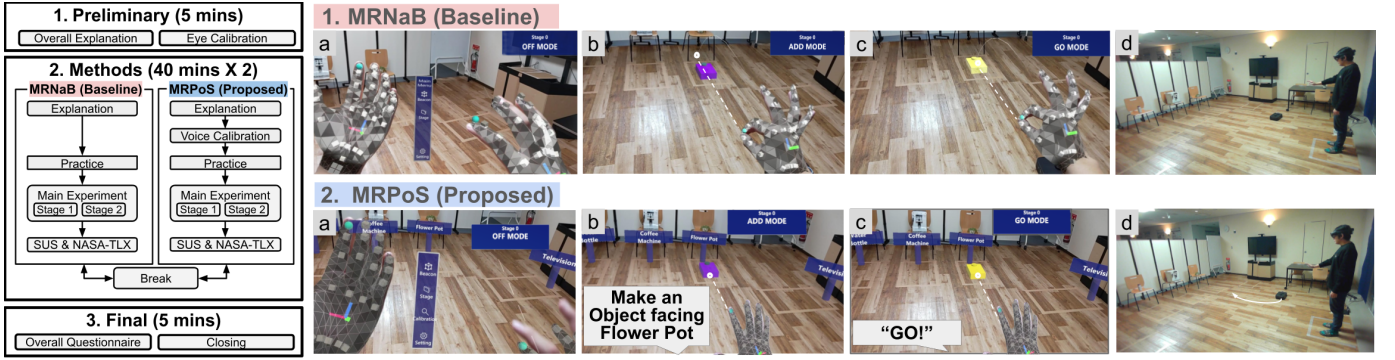


Fig. 11: **Overall Experiment Flow** comparing MRNaB and MRPoS. Upper image shows the experiment flow while the lower image shows the main experiment flow. Both groups access the hand menu to generate the initial objects. Next, MRNaB employs hand gestures to instantiate and select MR-beacon. In contrast, MRPoS utilizes speech and spatial pointing to create and select MR-beacon. Once selected, robot starts the navigation.

The experiment consisted of two distinct stages. Stage 1 required participants to navigate to a single target, the tissue box, positioned at an oblique angle of  $210^\circ$ . This stage was specifically designed to evaluate the system’s performance in a challenging orientation that complicates MR-beacon generation. In contrast, Stage 2 involved a sequential navigation task to three locations: the chair, coffee machine, and TV. These targets were positioned at orthogonal angles ( $0^\circ$  or  $\pm 90^\circ$ ) to represent the more accessible configurations. This stage compared the proposed system’s efficiency against the baseline for multi-destination generation.

As shown in Fig. 11, both the baseline, MRNaB, and the proposed method began with a preparation phase, where participants watched an explanatory video and practiced with the system to familiarize themselves with its operation. Specifically for the proposed method, we also conducted voice calibration using example prompts with the format: “Make an object here facing {Place Name}”. However, they were permitted to customize the phrasing themselves. For the clustering logic in Section IV-D2, the distance threshold  $D_{th}$  was set to 0.15m to ensure stable MR-beacon generation. Fig. 11 also shows the main experiment of each methods by utilizing each modalities. Finally, each method experiment was concluded with the SUS and NASA-TLX questionnaires. At the end, participants filled in the overall questionnaire.

## B. Evaluation Indices

The evaluation metrics were categorized into two primary groups: objective and subjective indices. The objective metrics comprised three performance indicators: (1) the total time required for participants to generate all MR-beacons, (2) the cumulative count of *Add* and *Edit* actions performed to complete each stage, and (3) the location and rotation errors per MR-beacons from the predefined ground truth.

The subjective indices consisted of two primary metrics. First, system usability with System Usability Scale (SUS) questionnaire [30] and second, the system workload, measured by the NASA Task Load Index (NASA-TLX) [31].

To evaluate statistical significance, we first performed the Shapiro-Wilk test [32] to determine whether our data followed

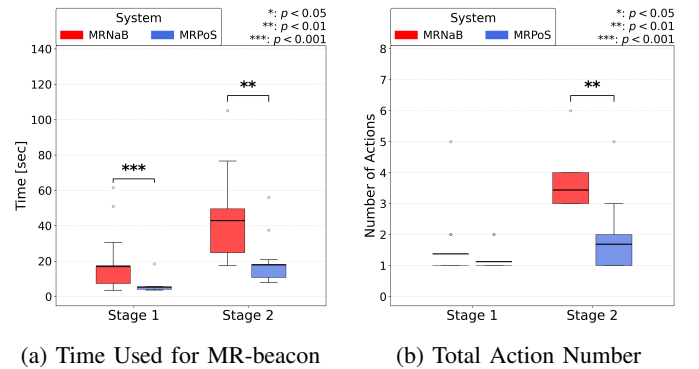


Fig. 12: **Time and Action Count Result**. Statistical difference on Stage 1 & 2 for time and on Stage 2 for action.

TABLE II: Time and Action Count Results

Stage	Time [sec]		Action Count	
	MRNaB	MRPoS	MRNaB	MRPoS
Stage 1	17.21	<b>5.37</b>	1.38	<b>1.12</b>
Stage 2	42.92	<b>17.88</b>	3.44	<b>1.69</b>

a normal distribution. For datasets that satisfied the normal distribution, we employed a Paired-Sample T-test [33], while for data that deviated from a normal distribution, we used the Wilcoxon Signed-Rank test [34].

## C. Experiment Result

1) *Time Used to Create Beacon*: The results, shown in Fig. 12a, demonstrate a statistically significant reduction in task completion time ( $p = 0.00076$  for Stage 1,  $p = 0.0012$  for Stage 2). As shown in Table II (left), participants using the proposed method finished the tasks significantly faster than those using the baseline. On average, our system required only 5.36 seconds for Stage 1 and 17.86 seconds for Stage 2. Conversely, the baseline system averaged 17.21 seconds and 42.92 seconds for Stage 1 and 2. We posit that this substantial increase in time stems from our interface enabling both single-

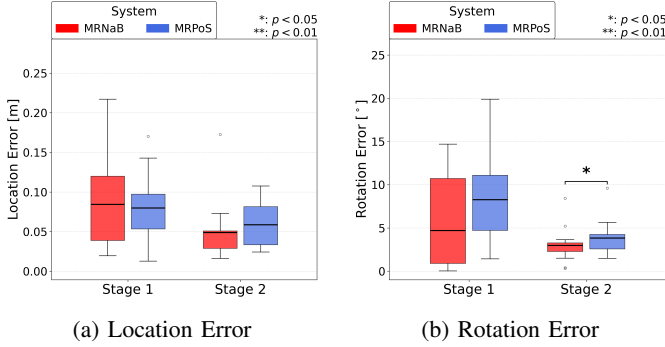


Fig. 13: **Location and Rotation Error per MR-beacon Result.**

TABLE III: Location and Rotation Error

Stage	Location Error [m]		Rotation Error [°]	
	MRNaB	MRPoS	MRNaB	MRPoS
Stage 1	0.084	<b>0.080</b>	<b>4.70</b>	8.27
Stage 2	<b>0.049</b>	0.059	<b>2.98</b>	3.83

step goal pose generation and the concurrent placement of multiple MR-beacons.

2) *Action Count Needed*: The results, shown in Fig. 12b, demonstrate a reduction in the required number of *Add* and *Edit* as the primary interactive effort, especially in multiple places condition, achieving statistical significance in the second stage ( $p = 0.0022$  for Stage 2). As shown in Table II (right), participants using the proposed method required fewer actions to create the MR-beacons than those using the baseline. On average, our system required only 1.12 actions for Stage 1 and 1.69 actions for Stage 2. Conversely, the baseline system averaged 1.38 actions and 3.44 actions for the respective stages. We posit that this substantial decrease in required actions stems from our interface enabling the concurrent placement of multiple MR-beacons.

3) *Location and Rotation Error per MR-beacon*: The results, shown in Fig. 13, demonstrate a statistically significant difference only for rotation error during Stage 2 ( $p = 0.013$ ). As summarized in Table III, proposed method yielded a significant difference compared to the baseline MRNaB system exclusively in rotation. We attribute these results to the fact that, for MRPoS, rotation is derived from both the MR-beacon and MR-label locations introducing additional variables which increases error in rotation.

4) *SUS and NASA-TLX*: The subjective evaluation results, illustrated in Fig. 14 and summarized in Table IV, demonstrate a statistically significant reduction in user workload for the proposed MRPoS system compared to the MRNaB baseline ( $p = 0.013$ ). This improvement represents a large effect size ( $r = 0.620$ ), suggesting a substantial decrease in the cognitive and physical demands of the task. Furthermore, the SUS scores indicated a marginal trend toward improved usability ( $p = 0.064$ ) with a substantial medium-to-large effect size ( $r = 0.464$ ). We attribute these findings to the multimodal nature of MRPoS by integrating speech and pointing, the

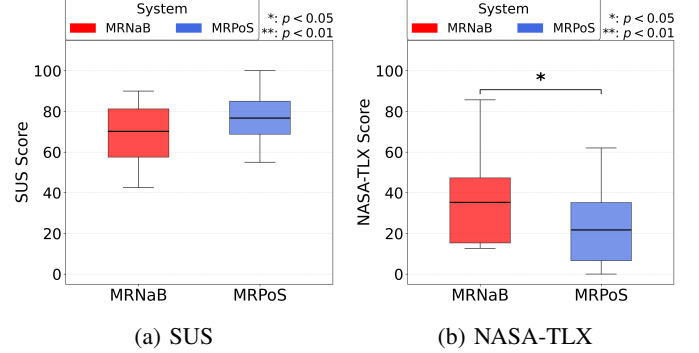


Fig. 14: **SUS and NASA-TLX Result.** Statistical difference can be found for NASA-TLX

TABLE IV: Statistical Analysis of Subjective Metrics (SUS and NASA-TLX)

Metric	MRNaB	MRPoS	$p$ -value	Effect Size
SUS Score $\uparrow$	70.16	<b>76.72</b>	0.064	0.464
NASA-TLX $\downarrow$	35.27	<b>21.67</b>	0.013	0.620

TABLE V: MRPoS Time Breakdown [sec]

Stage	Voice	STT	LLM	Clustering	Overall
Stage 1	4.20	0.35	0.81	0.01	<b>5.37</b>
Stage 2	15.72	0.75	1.39	0.02	<b>17.88</b>

system requires less time and fewer discrete actions while eliminating the need for complex hand gestures, thereby lowering the overall barrier to interaction.

#### D. Discussion

Table V shows that the proposed method outperformed the baseline in both completion time and action count. This improvement stems from the LLM’s ability to resolve degraded STT output, such as “An object here facing a Tish box”, which would otherwise fail. The decrease in time also means less time to raise hands resulting in lower workload shown in Table IV. Table V demonstrates that the combined STT and LLM latency remains within 1–2 seconds, varying slightly with the complexity of the input. This low-latency performance minimizes the perceived delay, facilitating real-time responsiveness for the MRPoS interface.

Another notable result in Table III is the difference in rotational error between MRNaB and MRPoS, which was higher in Stage 1 than in Stage 2. This discrepancy is largely attributable to the experimental setup of Stage 1. Despite only a single target, the location was positioned at an oblique angle ( $210^\circ$ ) in an area with limited visibility, which likely reduced participants’ precision when matching with the MR-label to create MR-beacons. However, even with this slight rotational variance, the proposed method proved to be significantly more efficient overall.

## VI. CONCLUSION

This paper proposes MRPoS, a Mixed Reality-based robot navigation interface that leverages spatial pointing and LLM-processed speech to simultaneously define the positions and orientations of multiple MR-beacons. The system features four primary functions, which are Add, Edit, Go, and Delete, enabling users to seamlessly generate single or multiple MR-beacons in a single action, modify their location and rotation, transmit the MR-beacon data to the physical robot to initiate autonomous navigation, and remove unwanted MR-beacons.

To evaluate MRPoS, we conducted a comparative experiment against the “air tap” based MR interface, MRNaB. Objective results showed that MRPoS achieved faster task completion with significantly fewer attempts. Furthermore, subjective evaluations confirmed a lower mental workload, validating MRPoS as a more efficient navigation interface.

## REFERENCES

- [1] M. Quigley, K. Conley, B. Gerkey, J. Faust, T. Foote, J. Leibs, R. Wheeler, and A. Y. Ng, “Ros: an open-source robot operating system,” in *ICRA workshop on open source software*, vol. 3, no. 3.2. Kobe, Japan, 2009, p. 5.
- [2] Y. Bisk, A. Holtzman, J. Thomason, J. Andreas, Y. Bengio, J. Chai, M. Lapata, A. Lazaridou, J. May, A. Nisnevich, N. Pinto, and J. Turian, “Experience Grounds Language,” in *Proceedings of the 2020 Conference on Empirical Methods in Natural Language Processing (EMNLP)*. Association for Computational Linguistics, Nov. 2020, pp. 8718–8735.
- [3] N. Hirose, C. Glossop, D. Shah, and S. Levine, “Omnivla: An omni-modal vision-language-action model for robot navigation,” *arXiv:2509.19480*, Sep. 2025.
- [4] J. D. Hincapié-Ramos, X. Guo, P. Moghadasian, and P. Irani, “Consumed Endurance: A Metric to Quantify Arm Fatigue of Mid-Air Interactions,” in *Proceedings of the SIGCHI Conference on Human Factors in Computing Systems*. ACM, 2014, pp. 1063–1072.
- [5] K. Owaki, N. Techasartikul, and H. Shimonishi, “Human Behavior Analysis in Human-Robot Cooperation with AR Glasses,” in *Proc. of the IEEE International Symposium on Mixed and Augmented Reality*. Los Alamitos, CA, USA: IEEE Computer Society, 2023, pp. 20–28.
- [6] M. Walker, H. Hedayati, L. Lee, and D. Szafr, “Communicating Robot Motion Intent with Augmented Reality,” in *Proc. of the ACM/IEEE International Conference on Human-Robot Interaction*, 2018, pp. 316–324.
- [7] T. Taki, M. Kobayashi, E. Iglesias, N. Chiba, S. Shirai, and Y. Uranishi, “Mrhad: Mixed reality-based hand-drawn map editing interface for mobile robot navigation,” in *2025 34th IEEE International Conference on Robot and Human Interactive Communication (RO-MAN)*, 2025, pp. 1888–1895.
- [8] J. Lee, T. Lim, and W. Kim, “Investigating the usability of collaborative robot control through hands-free operation using eye gaze and augmented reality,” in *2023 IEEE/RSJ International Conference on Intelligent Robots and Systems (IROS)*, 2023, pp. 4101–4106.
- [9] E. Iglesias, M. Kobayashi, Y. Uranishi, and H. Takemura, “Mrnab: mixed reality-based robot navigation interface using optical-see-through mr-beacons,” *Advanced Robotics*, vol. 39, no. 11, pp. 663–677, 2025. [Online]. Available: <https://doi.org/10.1080/01691864.2025.2508779>
- [10] K. C. Hoang, W. P. Chan, S. Lay, A. Cosgun, and E. A. Croft, “ARviz: An Augmented Reality-Enabled Visualization Platform for ROS Applications,” *IEEE Robotics & Automation Magazine*, vol. 29, no. 1, pp. 58–67, 2022.
- [11] R. C. Quesada and Y. Demiris, “Holo-SpoK: Affordance-Aware Augmented Reality Control of Legged Manipulators,” in *Proc. of the IEEE/RSJ International Conference on Intelligent Robots and Systems*, 2022, pp. 856–862.
- [12] P. Yu, A. Arora, Y. Song, and G. Soh, “A mixed reality platform for online motion planning of mobile robots via hololens 2,” 01 2022, pp. 817–820.
- [13] A. Angelopoulos, A. Hale, H. Shaik, A. Paruchuri, K. Liu, R. Tuggle, and D. Szafr, “Drone Brush: Mixed Reality Drone Path Planning,” in *Proc. of the ACM/IEEE International Conference on Human-Robot Interaction*, 2022, pp. 678–682.
- [14] C. Cruz, J. Cerro, and A. Barrientos, “Mixed-reality for quadruped-robotic guidance in SAR tasks,” *Journal of Computational Design and Engineering*, vol. 10, 2023.
- [15] P. S. Garcia, P. Lukovic, L. Reynaud, A. Sgobbi, F. Bruni, M. Brun, M. Zünd, R. Bollati, M. Pollefeys, H. Blum, and Z. Bauer, “Holospot: Intuitive object manipulation via mixed reality drag-and-drop,” *arXiv:2410.11110*, Oct. 2024.
- [16] T. Engelbracht, P. Lukovic, T. Behrens, K. Lascheit, R. Zurbrügg, M. Pollefeys, H. Blum, and Z. Bauer, “Spot-on: A mixed reality interface for multi-robot cooperation,” *arXiv:2505.22539*, May 2025.
- [17] J. Chen, B. Sun, M. Pollefeys, and H. Blum, “A 3d mixed reality interface for human-robot teaming,” in *2024 IEEE International Conference on Robotics and Automation (ICRA)*, 2024, pp. 11 327–11 333.
- [18] G. Zhang, L. Duan, and G. Han, “Accessible Robot Control in Mixed Reality,” *arXiv preprint arXiv:2306.02393*, 2023, available: [arXiv:2306.02393 \[cs.RO\]](https://arxiv.org/abs/2306.02393).
- [19] A. Payandeh, D. Song, M. Nazeri, J. Liang, P. Mukherjee, A. H. Raj, Y. Kong, D. Manocha, and X. Xiao, “Social-llava: Enhancing social robot navigation through human-language reasoning,” in *2025 IEEE/RSJ International Conference on Intelligent Robots and Systems (IROS)*, 2025, pp. 17 192–17 198.
- [20] C. Wen, Y. Liu, G. C. R. Bethala, S. Yuan, H. Huang, Y. Hao, M. Wang, Y.-S. Liu, A. Tzes, and Y. Fang, “Socially-aware robot navigation enhanced by bidirectional natural language conversations using large language models,” *arXiv preprint arXiv:2409.04965*, 2024.
- [21] S. Nikolaidis, M. Kwon, J. Forlizzi, and S. Srinivasa, “Planning with verbal communication for human-robot collaboration,” *J. Hum.-Robot Interact.*, vol. 7, no. 3, Nov. 2018. [Online]. Available: <https://doi.org/10.1145/3203305>
- [22] S. Song, S. Kodagoda, A. Gunatilake, M. G. Carmichael, K. Thiagarajan, and J. Martin, “Guide-llm: An embodied llm agent and text-based topological map for robotic guidance of people with visual impairments,” in *2025 International Conference on Sensing Techniques (ICST)*, 2025, accepted for publication.
- [23] K.-L. Chen, T.-T. Wei, L.-T. Yeh, E. Kao, Y.-C. Tseng, and J.-J. Chen, “Resolving positional ambiguity in dialogues by vision-language models for robot navigation,” *arXiv:2410.12802*, Oct. 2024.
- [24] S. Y. Gadre, M. Wortsman, G. Ilharco, L. Schmidt, and S. Song, “Cows on pasture: Baselines and benchmarks for language-driven zero-shot object navigation,” *CVPR*, 2023.
- [25] N. Hirose, C. Glossop, A. Sridhar, D. Shah, O. Mees, and S. Levine, “Lelan: Learning a language-conditioned navigation policy from in-the-wild video,” in *Conference on Robot Learning*, 2024.
- [26] C. Glossop, W. Chen, A. Bhorkar, D. Shah, and S. Levine, “Cast: Counterfactual labels improve instruction following in vision-language-action models,” *arXiv:2508.13446*, Aug. 2025.
- [27] X. Shi, Z. Li, W. Lyu, J. Xia, F. Dayoub, Y. Qiao, and Q. Wu, “Smartway: Enhanced waypoint prediction and backtracking for zero-shot vision-and-language navigation,” in *2025 IEEE/RSJ International Conference on Intelligent Robots and Systems (IROS)*, 2025, pp. 16 923–16 930.
- [28] W. Zu, W. Song, R. Chen, Z. Guo, F. Sun, Z. Tian, W. Pan, and J. Wang, “Language and sketching: An llm-driven interactive multimodal multitask robot navigation framework,” in *2024 IEEE International Conference on Robotics and Automation (ICRA)*, 2024, pp. 1019–1025.
- [29] Muhtadin, V. G. P. A. B. M., A. Zaini, M. H. Purnomo, I. K. E. Purnama, and C. Faticah, “Quadruped-legged robot movement plan generation using large language model,” *arXiv:2512.21293*, Dec. 2025.
- [30] J. Brooke, “SUS: A quick and dirty usability scale,” *Usability Eval. Ind.*, vol. 189, 1995.
- [31] S. G. Hart and L. E. Staveland, “Development of NASA-TLX (Task Load Index): Results of Empirical and Theoretical Research,” in *Human Mental Workload*. North-Holland, 1988, vol. 52, pp. 139–183.
- [32] S. S. Shapiro and M. B. Wilk, “An Analysis of Variance Test for Normality (Complete Samples),” *Biometrika*, vol. 52, no. 3/4, pp. 591–611, 1965.
- [33] W. S. Gosset, “The Probable Error of a Mean,” *Biometrika*, vol. 6, no. 1, pp. 1–25, 1908.
- [34] D. Rey and M. Neuhäuser, “Wilcoxon-Signed-Rank Test,” *International Encyclopedia of Statistical Science*, pp. 1658–1659, 2011.